

AB-INITIO STUDY OF MAGNETIC PROPERTIES OF ZnO:Cr AND ZnSnAs<sub>2</sub>:(V,Mn)G.S. ORUDZHEV<sup>1,2</sup>, V.N. JAFAROVA<sup>1</sup>, S.S. HUSEYNOVA<sup>1</sup><sup>1</sup>*Institute of Physics of ANAS, 131 H. Javid ave, Baku, AZ 1143, Azerbaijan*<sup>2</sup>*Azerbaijan Technical University, 25 H. Javid ave, Baku, AZ 1073, Azerbaijan**e-mail: vina246@rambler.ru*

We present a theoretical study of the structural, electronic and magnetic properties of Cr and V, Mn doped hexagonal ZnO and tetrahedrally bonded chalcopyrite ZnSnAs<sub>2</sub> semiconductors, respectively. Ab initio calculations were performed by the Density Functional Theory method using Atomistix Tool Kit program software within the Local Spin Density and Spin Generalized Gradient Approximations.

**Keywords:** ZnO, ZnSnAs<sub>2</sub>, ATK, ab initio calculation, Local Density Approximation, Spin Generalized Gradient Approximation ferromagnetism, magnetic moment.

**PACS:** 537.621.5, 548.4

## 1. INTRODUCTION

ZnO is a hexagonal material that crystallizes in the wurtzite structure [1]. ZnO with wide band gap has been identified as a promising direct band gap semiconductor material, exhibiting room temperature ferromagnetism when doped with 3d-transition metal ions (Cr, Co, Fe, Mn, Cr or V). Ferromagnetism in transition metal-doped ZnO is theoretically predicted in [2] using ab initio calculations based on density functional theory (DFT) local density approximation (LDA).

ZnSnAs<sub>2</sub> is a II-IV-V<sub>2</sub> tetrahedrally bonded chalcopyrite semiconductor with energy gap within 0.6-0.76 eV at 300 K [3]. The ZnSnAs<sub>2</sub>:Mn films grown on InP (001) substrates show a ferromagnetic phase exhibiting high Curie temperature ( $T_c=330$  K) [4-6]. This makes ZnSnAs<sub>2</sub> with 3d-elements incorporated a promising candidate for application in spintronics [7].

In this work we study the structural, electronic and magnetic properties of bulk and Cr-doped ZnO and V-, Mn-doped ZnSnAs<sub>2</sub> by using the ab-initio calculations. Also have been considered ferromagnetic and antiferromagnetic spin ordering of dopant Cr, V and Mn atoms. To simulate the doping effect we have performed our calculations for primitive cell and supercells of ZnO and ZnSnAs<sub>2</sub>, using Atomistix Tool Kit program software (ATK, <http://quantumwise.com/>) on based Density Functional Theory DFT [8] with local spin density approximation (LSDA) [9] and Spin Generalized Gradient Approximation (SGGA) [10], respectively. In so doing, we have been able to reproduce experimental value of energy gap only using Hubbard\_U corrections.

## 2. COMPUTATIONAL DETAILS

Our calculations were performed for the primitive cell of ZnO and ZnSnAs<sub>2</sub>, and for a number of supercells with as many atoms in the case of Cr-doped ZnO and V-, Mn- doped ZnSnAs<sub>2</sub> by implementing the DFT+U using the ATK programme software, within the LSDA and SGGA methods, respectively. The electron-ion interactions were taken into account through pseudopotentials of the Fritz Haber Institute (FHI). The Perdew-Burke-Ernzerhof (PBE) exchange-correlation functional [11] and Double Zeta Polarized basis sets were

used in ATK calculations. The kinetic cut-off energy was 150 Ry. The primitive cell of ZnO and ZnSnAs<sub>2</sub> was relaxed and optimized with force and stress tolerances of 0.01 eV/Å and 0.01 eV/Å<sup>3</sup>, respectively. The investigated supercells containing Cr-, V and Mn dopant atoms were relaxed with force tolerance of 0.05 eV/Å.

The magnetic moments calculations were done by Mulliken population analysis. The number of the electrons treated as valence electrons was 6 for 12 for Zn (3d<sup>10</sup>4s<sup>2</sup>), 6 for O (2s<sup>2</sup>2p<sup>4</sup>), Cr (3d<sup>5</sup>4s<sup>1</sup>), 5 for V (3d<sup>3</sup>4s<sup>2</sup>), 7 for Mn (3d<sup>5</sup>4s<sup>2</sup>), 4 for Sn (5s<sup>2</sup>5p<sup>2</sup>), and 5 for As (4s<sup>2</sup>4p<sup>3</sup>). The Hubbard U-parameter we used in our calculations for Cr-, V- and Mn-3d states were 2.32 eV, 2.73 eV and 3.02 eV, respectively.

## 3. RESULTS AND DISCUSSION

### 3.1. LATTICE PARAMETERS AND BAND STRUCTURES OF PURE ZnO and ZnSnAs<sub>2</sub> CRYSTALS

The optimized values of the lattice parameters ( $a$ ,  $c$ ) for ZnO are in a good agreement with theoretical [12] and experimental dates [12,13,14,15] (Table 1). The values of lattice parameters, anion displacement parameter ( $u$ ) and tetragonal distortion parameter ( $c/2a$ ) for ZnSnAs<sub>2</sub> are listed in Table 2 together with the relevant experimental results [16-18].

According to the ab initio obtained band structures (Figures 1 and 2) and the density of states of the pure ZnO and ZnSnAs<sub>2</sub> are a direct band gap non-magnetic semiconductors. Both the valence band top and conduction band bottom are located at the center of the Brillouin zone. The values of the energy gap of ZnO and ZnSnAs<sub>2</sub> compounds are 3.4 and 0.34 eV, respectively. Spin-up and spin-down states form the same band structure.

### 3.2. ZnO with Cr(Zn) substitution

A systematic study on the composition of dopant would yield a trend for the entire range of composition using in Cr-doped ZnO compound could be exploited for magneto-optical device application [19]. In [20] investigated the microstructure and the magnetic properties of Zn<sub>1-x</sub>Cr<sub>x</sub>O thin films deposited on quartz

glass substrates using radiofrequency magnetron sputtering.

The crystal structure and ferromagnetic spin polarization for  $Zn_{47}Cr_1O_{48}$  supercell contained one Cr(Zn) substitution is shown in Fig. 3. A would be

expected, doping ZnO with transition Cr atoms leads to a magnetization of the structure. This is related to the fact, that the partially filled *d* states of dopant Cr atoms contain unpaired electrons.

Table 1

A comparison between the calculated, other theoretical and experimental lattice parameters for ZnO.

Parametr	This work	Theor. [12]	Exp. [12]	Exp. [13]	Exp. [14]	Exp. [15]
<i>a</i> , Å	3.2495	3.238	3.258	3.249	3.250	3.275
<i>c</i> , Å	5.2069	5.232	5.220	5.206	5.204	5.247
<i>c/a</i>	1.60	1.62	1.60	1.60	1.60	1.60

Table 2

The calculated and experimental lattice parameters, the anion displacement parameter and the tetragonal distortion parameter for  $ZnSnAs_2$ .

Parameters	This work	Ref. [16]	Ref. [17]	Ref.[18]
<i>a</i> , Å	5.836	5.852	5.853	5.85
<i>c</i> , Å	11.776	11.703	11.712	11.70
<i>c/2a</i>	1.010	1.000	1.000	1.00
<i>u</i>	0.2315	0.231	-	0.231

Table 3.

The calculated values of the magnetic moment per one dopant Cr atom for different supercells with two Cr(Zn) substitutions.

Supercell	Number of atoms	x	$\mu/Cr$ (in $\mu_B$ )
$Zn_{22}Cr_2O_{24}$	48	1/12	3.97
$Zn_{46}Cr_2O_{48}$	96	1/24	3.96
$Zn_{62}Cr_2O_{64}$	128	1/32	3.96
$Zn_{94}Cr_2O_{96}$	192	1/48	3.96

Table 4.

The calculated values of the magnetic moment per one dopant V atom for different supercells with two V(Zn) substitutions.

Supercell	Number of atoms	<i>x</i>	$\mu/V$ (in $\mu_B$ )
$Zn_6Sn_8V_2As_{16}$	32	1/8	3.00
$Zn_{10}Sn_{12}V_2As_{24}$	48	1/12	3.00
$Zn_{14}Sn_{16}V_2As_{32}$	64	1/16	3.00
$Zn_{22}Sn_{24}V_2As_{48}$	96	1/24	3.00
$Zn_{30}Sn_{32}V_2As_{64}$	128	1/32	2.99
$Zn_{46}Sn_{48}V_2As_{96}$	192	1/48	3.00
$Zn_{62}Sn_{64}V_2As_{128}$	256	1/64	3.00

Table 5.

The calculated values of the magnetic moment per one dopant V atom for different supercells with two V(Zn) substitutions.

Supercell	Number of atoms	<i>x</i>	$\mu/V$ (in $\mu_B$ )
$Zn_8Sn_6V_2As_{16}$	32	1/8	1.00
$Zn_{12}Sn_{10}V_2As_{24}$	48	1/12	0.997
$Zn_{16}Sn_{14}V_2As_{32}$	64	1/16	0.998
$Zn_{24}Sn_{22}V_2As_{48}$	96	1/24	0.999
$Zn_{32}Sn_{30}V_2As_{64}$	128	1/32	1
$Zn_{48}Sn_{46}V_2As_{96}$	192	1/48	0.997
$Zn_{64}Sn_{62}V_2As_{128}$	256	1/64	0.997

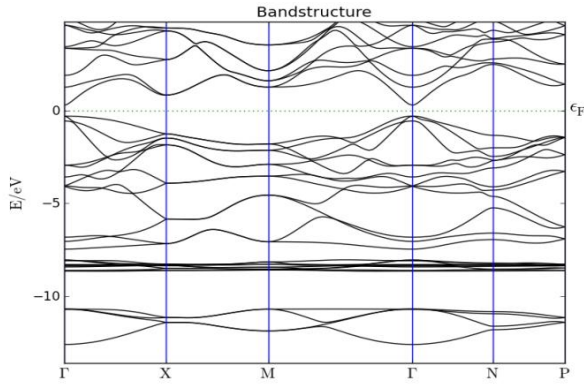


Fig. 1. Ab-initio calculated band structure for ZnO.

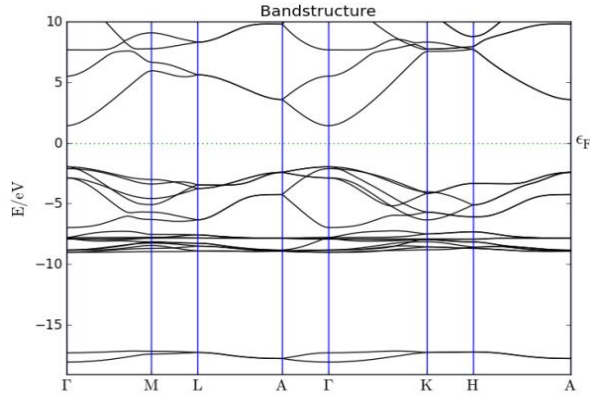


Fig. 2. Ab-initio calculated band structure for ZnSnAs<sub>2</sub>.

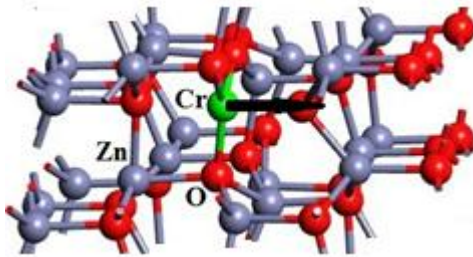


Fig. 3. Spin polarization of Zn<sub>47</sub>Cr<sub>1</sub>O<sub>48</sub>. The magnetic moment of Cr-3d dopant atoms are shown by black axes.

In case of Cr(Zn) substitution, the values of the magnetic moment per Cr atom, derived from the Mulliken population analysis, are given in Table 3. As seen from Table 3, the magnetic moment in all the studied supercells is the same and weakly depending on the dopant concentration.

The results of the total energy calculations for Zn<sub>1-x</sub>Cr<sub>x</sub>O supercells with x=1/12, 1/24, 1/32 and 1/48 show that a ferromagnetic ordering in Cr-doped ZnO when Cr replaces Zn. It is rather straight forward that doping of ZnO with transition Cr atoms which have the unpaired electrons in the incompletely filled Cr-3d orbitals would lead to the magnetization of the structure and

the calculation of the emerging magnetization makes sense.

### 3.3. ZnSnAs<sub>2</sub> supercell with V(Zn) substitution

The crystal structure and ferromagnetic spin polarization for Zn<sub>23</sub>Sn<sub>24</sub>V<sub>1</sub>As<sub>48</sub> supercell contained one V(Zn) substitution is shown in Figure 4. In case of V(Zn) substitution, the calculated magnetic moment of the 96-atoms supercell ( $3\mu_B$ ) is mainly determined by the magnetic moment of the dopant ( $2.963\mu_B$  from V atom including basically  $2.797\mu_B$  from d-electrons). The negative magnetic moment of all As atoms is small in magnitude ( $-0.107\mu_B$ ) and almost compensated by the positive moment created in common by Zn and Sn atoms. In case of two V(Sn) substitutions, the calculated values of the magnetic moment, derived from the Mulliken population analysis, are given in Table 4.

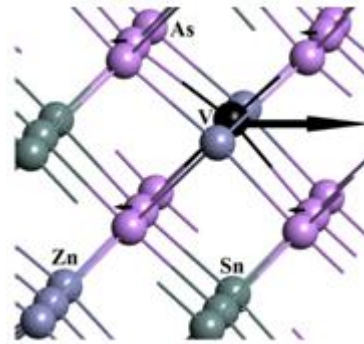


Fig. 4. V(Zn) substitution and its neighborhood in the Zn<sub>23</sub>Sn<sub>24</sub>V<sub>1</sub>As<sub>48</sub> supercell. The calculated magnetic moments of atoms are shown by black axes.

Mulliken population analysis shows that in the magnetization along with dopant V atom participate also As atoms, by weakening the overall magnetization. The main negative contributions in this case belong to 4 As atoms, which have chemical bonding with dopant V atom. Note that, the magnetic moment of As atoms are formed due to their *p*-orbitals. Participation of Zn and Sn atoms in the magnetization is negligible (total  $\sim 0.1\mu_B$  for each type of atoms). By a single V(Zn) substitution in the 96-atoms supercell occurs total magnetic moment of  $3.0\mu_B$ .

### 3.4. ZnSnAs<sub>2</sub> with V(Sn) substitution

Figure 5 displays the V atom and its neighborhood in the Zn<sub>24</sub>Sn<sub>23</sub>V<sub>1</sub>As<sub>48</sub> supercell. The calculated total magnetic moment per one dopant vanadium atom is  $0.999\mu_B$ . The main partial magnetic moments are distributed among the atoms as follows:  $2.151\mu_B$  from V atom, including basically  $2.077$  from d,  $-1.028\mu_B$  from 48 As atoms. In fact, only 4 As atoms which are chemically bonded to the dopant V give considerable negative contribution ( $-0.754\mu_B$ ) into the total magnetic moment. It is found, that in V(Sn) substitution case a ferromagnetic spin ordering is more stable compared with an antiferromagnetic one. In case of two V(Sn) substitutions, the calculated values of the magnetic moment, derived

from the Mulliken population analysis, are given in Table 5.

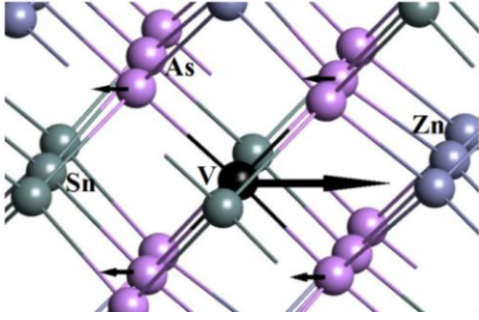


Fig. 5. V(Sn) substitution and its neighborhood in the  $Zn_{24}Sn_{23}V_1As_{48}$  supercell. The magnetic moments of atoms are shown by black axes.

This is due to the fact that, in case of V(Zn) substitution As-atoms weakens the field much less and the magnetic moment created by V-atom is more  $0.812 \mu_B$  as compared to the V(Sn) substitution.

### 3.5. $ZnSnAs_2$ supercell with Mn(Sn) substitution

The results of the total energy calculations for  $ZnSn_{1-x}Mn_xAs_2$  supercells with  $x=1/8, 1/16, 1/24$  and  $1/32$  show that a ferromagnetic rather than antiferromagnetic ordering is favorable in Mn-doped  $ZnSnAs_2$  when Mn replaces Sn. The values of the magnetic moment per Mn atom, derived from the Mulliken population analysis, are

given in Table 6. As seen from the Table 6, the magnetic moment in all the studied supercells is around  $3 \mu_B$ .

For comparison, the magnetic moment determined from the saturation magnetization studies is  $3.63 \mu_B$  at 5 K for  $x=0.0125$  [4]. In the 5% and 7% Mn-doped  $ZnSnAs_2$  thin films the magnetic moments per Mn atom at 5 K are approximately  $0.87$  and  $2.75 \mu_B$ , respectively [5]. Mn-doped properties of  $ZnSnAs_2$  by the first-principles calculations shown that, in case of Mn doping at Sn sites, when Mn atoms are isolated, each Mn atom induces a large spin moment around  $3.1 \mu_B$  per a single Mn atom, which merits the spintronics application. However, when the doping concentration increases and Mn atoms produce a neighboring pair, the spin moment decreases by the antiferromagnetic interaction between Mn atoms [21].

Our calculations show that at least for  $x < 0.15$  the energy gap of  $ZnSn_{1-x}Mn_xAs_2$  increases with increasing Mn concentration. For  $x < 0.03$  the gap increases linearly at a rate of  $2.05 eV$ .

Figure 6 shows positions of the Mn and neighboring Zn, Sn and As atoms in the  $Zn_{24}Sn_{23}Mn_1As_{48}$  supercell with the calculated total magnetic moment of  $3.088 \mu_B$ . The partial magnetic moments are distributed among the atoms as follows:  $4.747 \mu_B$  from Mn atom, including  $4.44$  from d,  $0.19$  from p and  $0.12 \mu_B$  from s states;  $-0.018 \mu_B$  from 24 Zn atoms;  $-0.008 \mu_B$  from 23 Sn atoms;  $-1.635 \mu_B$  from 48 As atoms. In fact, only 4 As atoms chemically bonded to Mn considerably contribute into the total moment. The contribution of the rest As atoms is negligible.

Ab-initio calculated values of magnetic moment per doping atoms for  $ZnSnAs_2$ : Mn.

Supercell	Number of atoms	$x$	$\mu/Mn$ (in $\mu_B$ )
$Zn_{16}Sn_{14}Mn_2As_{32}$	64	1/8	3.10
$Zn_{24}Sn_{22}Mn_2As_{48}$	96	1/12	3.09
$Zn_{32}Sn_{30}Mn_2As_{64}$	128	1/16	3.00
$Zn_{48}Sn_{46}Mn_2As_{96}$	192	1/24	2.99
$Zn_{64}Sn_{62}Mn_2As_{128}$	256	1/32	2.99

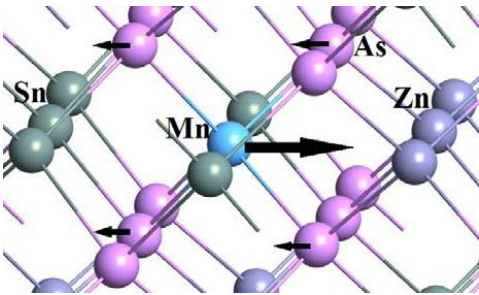


Fig. 6. Mn(Sn) substitution and its neighborhood in the  $Zn_{24}Sn_{23}Mn_1As_{48}$  supercell. The calculated magnetic moments of atoms are shown by black axes.

Note that, the calculated total energy difference between the AFM and FM states increases with increasing Mn concentration. In case of Mn(Sn) substitution the ferromagnetic (FM) spin ordering is favorable in

Table 6.

$ZnSnAs_2$ :Mn. The ab initio investigations show that the substitution Mn(Zn) led to the antiferromagnetic (AFM) spin ordering.

## 4. CONCLUSION

Ab initio calculations performed for a 32-, 48-, 64-, 96-, 128-, 192- and 256-atoms ZnO and  $ZnSnAs_2$  supercells. Due to the ab initio obtained band structures and density of states of the pure ZnO and  $ZnSnAs_2$  compounds are a direct band gap non-magnetic semiconductors. Mulliken population analysis shows that, when Cr(Zn) substitution in ZnO and V(Zn,Sn), Mn(Sn) substitutions in  $ZnSnAs_2$  lead to a ferromagnetic spin ordering. Note that, the doping of ZnO and  $ZnSnAs_2$  with the transient Cr and V, Mn atoms would lead to the magnetization of the structure, because of the unpaired electrons in the partially filled Cr- and V-, Mn-3d orbitals. The main negative contributions in Cr(Zn) substitution in

ZnO case belong to 4 O atoms, which have chemical bonding with dopant Cr atom. Participation of Zn and O atoms in the magnetization is negligible. By a single Cr(Zn) substitution in ZnO 96-atoms supercell occurs total magnetic moment of 3.384  $\mu_B$ . Ab initio calculations show that Zn and Sn substitutions by V in ZnSnAs<sub>2</sub> 96-atoms supercell both lead to a ferromagnetic spin ordering. According to the total energy calculations V(Sn) and

Mn(Sn) substitutions in ZnSnAs<sub>2</sub>:Mn are energetically favorable in comparison with V(Zn) and Mn(Zn).

#### ACKNOWLEDGEMENTS

This work was partly supported by the Science Development Foundation under the President of the Republic of Azerbaijan-grant No EIF-BGM-2-BRFTF-1-2012/2013-07/03/1-M-05.

- 
- [1] *T. Makino, Y. Segawa, M. Kawasaki et al.* Appl. Phys. Lett. 78, 1237, 2001
- [2] *K. Sato and H. Katayama-Yoshida.* Jpn. J. Appl. Phys. 39, L555, 2000
- [3] *V. Brudnyi, T. Vedernikova.* Russian Journal of Phys. Techn. Semicon. 43, 433, 2009
- [4] *S. Choi, G. Cha, S. Hong et al.* Solid State Communications. 122, 165, 2002
- [5] *N. Uchitomi, H. Oomae, J. Asubar, H. Endo and Y. Jinbo.* Jpn. J. Appl. Phys. 50, 05FB02-1, 2011
- [6] *J. Asubar, Y. Jinbo, N. Uchitomi.* Journal of Crystal Growth. 311, 929, 2009
- [7] *G. Medvedkin, T. Ishibashi, T. Nishi, K. Hayata, Y. Hasegawa and K. Sato.* Jpn. J. Appl. Phys. 39, L949, 2000
- [8] *P. Hohenberg, Kohn W.* Phys. Rev., 136, B864, 1964
- [9] *V.V. Karasiev, T. Sjostrom, J.W. Dufty, S.B. Trickey.* Phys. Rev. Lett. 112, 076403, 2014
- [10] *J. Perdew, J. Tao, V. Staroverov and G. Scuseria.* J. Chem. Phys. 120, 6898, 2004
- [11] *J. Perdew, K. Burke, M. Ernzerhof.* Phys. Rev. Lett., 77, 3865, 1996
- [12] *C. Jin, Y. Yang et al.* J. Mater. Chem. C, 2, 2992, 2014
- [13] *A. Arif, O. Belahssen et al.* J. of Semicon., 36, 013001-1, 2015
- [14] *F. Decremps, F. Datchi et al.* Phys. Rev. B, 68, 104101, 2003
- [15] *T. Malaeru, J. Neamtu et al.* Rev. Roum. Chim. 57, 857, 2012
- [16] *D. Gasson, P. Holmes, I. Jennings, B. Marathe, and J. Parrot.* J. Phys. Chem. Solids 23, 1291, 1962
- [17] *A. Vaipolin.* Sov. Phys. - Fiz. Tverd. Tela 15, 1430, 1973
- [18] *A. Mejidov, R. Muradov, X. Xalilova, and T. Mextiev.* Trans. Ser. Phys.-Math. Tech. Sci., Physics and Astronomy 2, 110, 2004
- [19] *D. Paul Joseph and C. Venkateswaran.* J. of Atomic, Molecular, and Optical Phys. 2011, 1, 2011
- [20] *L. Zhuge, X. Wu et al.* Scripta Materialia, 60, 214, 2009
- [21] *M. Ishikawa and T. Nakayama.* Phys. Status Solidi C 12, 6, 814, 2015

Received: 02.05.2017